Research Paper

Soluble Gamma-secretase Modulators Attenuate Alzheimer's β-amyloid Pathology and Induce Conformational Changes in Presenilin 1

CrossMark

Frank Raven [a,b,1], Joseph F. Ward [a,1], Katarzyna M. Zoltowska [c], Yu Wan [a,d], Enjana Bylykbashi [a], Sean J. Miller [a], Xunuo Shen [a], Se Hoon Choi [a], Kevin D. Rynearson [e], Oksana Berezovska [c], Steven L. Wagner [e,f,*], Rudolph E. Tanzi [a,*], Can Zhang [a,**]

[a] Genetics and Aging Research Unit, MassGeneral Institute for Neurodegenerative Diseases (MIND), Department of Neurology, Massachusetts General Hospital, Harvard Medical School, Charlestown, MA 02129-2060, USA
[b] Groningen Institute for Evolutionary Life Sciences, University of Groningen, Groningen 9747 AG, The Netherlands
[c] Alzheimer Research Unit, MassGeneral Institute for Neurodegenerative Diseases (MIND), Department of Neurology, Massachusetts General Hospital, Harvard Medical School, Charlestown, MA 02129-2060, USA
[d] Department of Neurology, Qingdao Municipal Hospital, Qingdao University, PR China
[e] Department of Neurosciences, University of California, La Jolla, San Diego, CA 92093-0624, USA
[f] Research Biologist, VA San Diego Healthcare System, La Jolla, CA, 92161, United States

ARTICLE INFO

ABSTRACT

A central pathogenic event of Alzheimer's disease (AD) is the accumulation of the Aβ42 peptide, which is generated from amyloid-β precursor protein (APP) via cleavages by β- and γ-secretase. We have developed a class of soluble 2-aminothiazole γ-secretase modulators (SGSMs) that preferentially decreases Aβ42 levels. However, the effects of SGSMs in AD animals and cells expressing familial AD mutations, as well as the mechanism of γ-secretase modulation remain largely unknown. Here, a representative of this SGSM scaffold, SGSM-36, was investigated using animals and cells expressing FAD mutations. SGSM-36 preferentially reduced Aβ42 levels without affecting either α- and β-secretase processing of APP nor Notch processing. Furthermore, an allosteric site was identified within the γ-secretase complex that allowed access of SGSM-36 using cell-based, fluorescence lifetime imaging microscopy analysis. Collectively, these studies provide mechanistic insights regarding SGSMs of this class and reinforce their therapeutic potential in AD.

© 2017 The Authors. Published by Elsevier B.V. This is an open access article under the CC BY-NC-ND license (http://creativecommons.org/licenses/by-nc-nd/4.0/).

1. Introduction

Alzheimer's disease (AD) is a devastating neurodegenerative disorder and the leading cause of dementia. There is currently no treatment available to slow or halt disease progression. The underlying mechanisms of AD on the cell and molecular levels are still not completely elucidated. Considerable genetic, pathological, biochemical, and molecular biological evidence supports the amyloid-cascade hypothesis, stating that the production and excessive accumulation of a small peptide, amyloid-β (Aβ), is the primary pathological event leading to AD (Gandy, 2005; Hardy and Selkoe, 2002; Tanzi and Bertram, 2005). Specifically, the accumulation of Aβ, particularly the neurotoxic Aβ42 peptide, affects neuronal synaptic functions and triggers an inflammatory response which is followed by neuritic injury and the generation of pathological tau proteins, ultimately leading to neuronal dysfunction and cell death.

AD is a genetically complex disease. Four AD genes (APP, PSEN1, PSEN2 and APOE) have been identified which primarily serve to increase the ratio of Aβ42 to Aβ40 or in the case of the Swedish mutation, absolute Aβ peptide levels. The imbalance triggered by these genetic aberrations enhances the oligomerization of Aβ into neurotoxic assemblies and ultimately leads to dementia (Bertram and Tanzi, 2008; Choi et al., 2014; Tanzi and Bertram, 2005). In the amyloidogenic pathway, Aβ is produced via sequential proteolytic cleavage of the type I transmembrane protein, amyloid-β (A4) precursor protein (APP) by β- and γ-secretase, respectively (Bertram and Tanzi, 2008; Zhang and Saunders, 2007). γ-Secretase is a heterogeneous protein complex, formed by at least four transmembrane proteins: presenilin (PS1), presenilin enhancer 2 (PEN2), nicastrin, and anterior pharynx-defective 1(APH-1) (Bertram and Tanzi, 2008; Edbauer et al., 2003; Sisodia and St George-Hyslop, 2002). Over 200 mutations in the PS1-encoding gene (PSEN1) have been identified to cause early-onset familial AD

(EOFAD), underscoring the relevance of the enzyme with respect to the disease. γ-Secretase regulates the intramembrane proteolysis of APP and numerous other substrates that have previously undergone ectodomain shedding, including Notch (Gu et al., 2004; Kopan and Ilagan, 2004; Sisodia and St George-Hyslop, 2002). The processing of Notch at the ε-site (or s3) represents a critical function of γ-secretase which yields a large cytoplasmic peptide, the Notch intracellular domain (NICD), which can translocate to the nucleus and is essential for cellular differentiation and development (Herreman et al., 1999; Kopan et al., 1994).

One essential strategy for AD therapeutics has focused specifically on APP processing and attenuating Aβ production (Bertram and Tanzi, 2008; Selkoe, 2001; Zhang, 2012, 2017). Initially, a class of drugs known as γ-secretase inhibitors (GSIs), were developed which potently inhibit γ-secretase activity. Despite the ability to preclude Aβ production, GSIs exhibit unfavorable activities that result in cell toxicity through increasing the levels of APP carboxy-terminal fragments (CTFs; CTFα and CTFβ), and side effects potentially elicited through down-regulation of Notch processing (Mitani et al., 2012). One of the well-characterized GSIs is semagacestat (or LY450139) (Doody et al., 2013; Mitani et al., 2012). Although it decreased the levels of all Aβ species (Potter et al., 2013), semagacestat recently failed in the pivotal phase 3 clinical trial for AD (Doody et al., 2013). Nevertheless, the results provide useful knowledge toward the features of a therapeutic for AD, which should avoid unfavorable adverse events associated with inhibition strategies in targeting either γ-, or β-secretease (De Strooper, 2014; Ward et al., 2017; Willem et al., 2015). Furthermore, this result provides evidence for a general need of improved understanding with respect to the critical biological roles of γ-secretase especially within the context of therapeutic development (De Strooper, 2014; Zhang, 2017).

A group of small molecule with a more promising therapeutic mechanism are known as γ-secretase modulators (GSMs), which modulate the cleavage activity of γ-secretase (and likely a host of other substrates) and specifically reduce the levels of the fibrillogenic Aβ42 peptide without altering the ε-site cleavage of APP or numerous other γ-secretase substrates, including Notch (Brendel et al., 2015; Imbimbo et al., 2007; Kounnas et al., 2010; Rogers et al., 2012). Since GSMs spare the ε-site processing of Notch, these compounds are considered likely to be safer and better tolerated than GSIs.

Previously, we reported the development and characterization of a series of GSMs with promising biological activities (Kounnas et al., 2010). The initial aminothiazole class of compounds displayed high potency for inhibiting the secretion of the Aβ42 peptide, however these compounds also suffered from poor aqueous solubility (Kounnas et al., 2010). Utilizing rational medicinal chemistry design, a class of aminothiazole GSMs was developed with improved physicochemical properties which include increased aqueous solubility and thus were referred to as soluble GSMs (or SGSMs)(Wagner et al., 2014). Importantly, these SGSMs were effective at reducing the levels of Aβ using cell-based models (D'Avanzo et al., 2015; Wagner et al., 2014). Further pharmacokinetic evaluation of this aminothiazole class of SGSMs in mice identified a lead compound, SGSM-36, which showed good brain penetration, as well as good clearance, half-life, and volume of distribution (Rynearson et al., 2016). These results collectively support the continued development of this class of compounds as a potential therapy for AD (Rynearson et al., 2016).

To advance our understanding of this aminothiazole class of compounds, further investigation using AD animal-based models and mechanistic studies were required to establish proof of concept in future clinical applications. Thus, in this study, we further characterized the representative aminothiazole SGSM with improved physicochemical properties for the potential effects on γ-secretase processing of APP in vivo using a well-studied AD mouse model, in addition to cell models of the disease. Furthermore, we investigated the effects of our representative aminothiazole SGSM on PS1 conformation using cell-based, fluorescence lifetime imaging microscopy (FLIM) analysis.

2. Materials and Methods

2.1. Animal Studies

All procedures conducted on animals were approved by MGH IACUC and conform to current animal welfare guidelines. The design and protocol followed our previous report (Kounnas et al., 2010). Briefly, Tg2576 mice which express human APP695 gene harboring the Swedish double mutation (KM670/671NL) were used (Hsiao et al., 1996; Kounnas et al., 2010). 3-Month old female Tg2576 mice were sourced from Taconic Biosciences (APPSWE; Model 1349) and used for short-term efficacy studies (n = 7 or n = 8 per group). Daily dosing was performed for three consecutive days by oral gavage in an 80% PEG 400 (v/v) vehicle. Three hours post drug administration on the last day, the animals were transcardially perfused under isoflurane anesthesia, blood was collected from mice via cardiac puncture into heparinized tubes. Whole blood was centrifuged (10,000 g for 10 min) to isolate plasma, aliquoted and stored at −80 °C for analysis. After brain dissection, tissue was processed for postmortem analyses, including biochemical studies.

2.2. Brain Extraction

Mouse brains were processed using previously reported methods (Kounnas et al., 2010; Veeraraghavalu et al., 2013, 2014). Briefly, brain hemispheres were homogenized in Tris-buffered saline (TBS) containing 1× Halt protease inhibitor cocktail (Thermoscientific) via polytron and applied to the following steps. Samples from the TBS homogenates were extracted with M-PER Mammalian Protein Extraction Reagent with 1× Halt protease inhibitor cocktail (Thermoscientific) and spun at 10,000 g for 20 min at 4 °C. The supernatant (MTBS) was used to detect total proteins, including membrane-bound proteins. In addition, TBS homogenates were spun at 100,000 g for 60 min at 4 °C. The supernatant was used to detect TBS soluble Aβ levels; and the pellets of TBS homogenates were further homogenized in 70% formic acid via polytron and spun at 100,000 g for 60 min. Finally, the supernatant of the formic acid extracts after centrifugation were used to detect TBS-insoluble Aβ levels. All samples were neutralized in 1 M Tris base buffer and then diluted before performing ELISA or Meso Scale analysis.

2.3. Cell Culture and Mouse Primary Cortical Neuron Culture

The Chinese hamster ovary CHO cell line stably expressing Indiana mutation in APP, also known as 7PA2 cells, has been previously reported (Walsh et al., 2002; Welzel et al., 2014). These cells were cultured and maintained on regular tissue culture plates in Dulbecco's modified Eagle's medium (DMEM) supplemented with 10% fetal bovine serum, 2 mM L-glutamine, 100 units per ml penicillin, 100 μg per ml streptomycin, and 200 μg/ml G418. Serum-free medium was utilized for experiments using 7PA2 cells. CHO cells stably expressing wild type APP751 and transiently transfected with the GFP-PS1-RFP FRET reporter has been previously reported (Uemura et al., 2009) and were used for the FLIM assay of PS1 conformational changes. Mouse primary neuronal cultures were prepared from cerebral cortex of CD-1 wild type mouse embryos at gestation day 16–18, as described previously (Berezovska et al., 1999). Briefly, the brain tissue was dissociated with Papain Dissociation Kit (Worthington Biochemical Corporation, Lakewood, NJ). The dissociated cells were plated on poly-D-lysine coated dishes and maintained in Neurobasal Medium supplemented with 2% B27, 1% Glutamax and 1% penicillin and streptomycin (ThermoScientific, Waltham, MA) in a 5% CO_2 incubator at 37 °C for 8–11 days in vitro (DIV).

The three-dimensional (3D) human neural cell culture and treatment were performed using the previously published protocol (Choi et al., 2014). Briefly, the HReN-mGAP cells expressing APP Swedish and London mutations and PSEN1 δE9 mutation were utilized. They were plated at a cell density of 20,000,000 cells per ml in a mixture of Matrigel and then 3D-differentiated for five weeks. Subsequently, cells

were treated with 400 nM SGSM-36 or vehicle (DMSO) for additional 2 weeks, and then medium was collected and applied to Aβ MSD analysis.

2.4. Reagents and Compounds

The GSI *N*-[*N*-(3,5-Difluorophenacetyl)-ʟ-alanyl]-(*S*)-phenylglycine *t*-butyl ester, also known as DAPT, was sourced from Tocris (catalog #: 2634). SGSM-36, *N*-(3-(*tert*-butyl)-1-ethyl-1*H*-pyrazol-5-yl)-4-(3-fluoro-4-(4-methyl-1*H*-imidazol-1-yl)phenyl)thiazol-2-amine, was designed at the University of California, San Diego and synthesized at Albany Molecular Research, Inc. (Albany, NY) and determined to be >95% pure based on liquid chromatography-tandem mass spectrometry and nuclear magnetic resonance analyses. SGSM-36 and close structural analogs also containing the 2-aminothiazole C-ring, have previously been investigated in cell culture-based studies (D'Avanzo et al., 2015). SGSM-36 was selected from the compounds within this particular family of aminothiazole-derived SGSMs based on good activity for attenuating Aβ42 and favorable physicochemical properties established by vigorous in vitro ADMET (absorption, distribution, metabolism, excretion, and toxicity) analysis to undergo further in vitro and in vivo studies (Rynearson et al., 2016).

2.5. Antibodies

The APP C-terminal polyclonal antibody (targeting the last 19 amino acids of APP) was purchased from Sigma (Catalog #: A8717) and the previously reported G12A antibody (Griciuc et al., 2013; Wang et al., 2015) were used to detect full length APP and APP-CTFs. The 6E10 antibody (Covance), a monoclonal antibody (mAb) reactive to amino acid residues 1–16 of Aβ from the N-terminal sequence, detects sAPPα and Aβ in the medium, as well as full length APP and APP-CTFβ in lysates. The mAb 22C11 was obtained from Millipore (Catalog #: MAB348) and active against residues 66–81 of APP from the N-terminal sequence. The polyclonal antibody sAPPβ was purchased from IBL (Catalog #: 18,957). The mAb Notch1 was obtained from Abcam (Catalog #: EP1238Y) and was produced by immunizing animals with a synthetic peptide corresponding to human Notch1 residues 2500–2600. It was used to detect the full length and cleaved Notch1 proteins. The PS1 N-terminal (NT) antibody (APS11), raised against PS1 N-terminus and the PS1 loop antibody (EP2000Y), raised against large cytosolic loop domain of PS1, were obtained from Abcam (Catalog #: ab15456 and ab76083, respectively). The PS1 C-terminal (CT) antibody, raised against PS1 C-terminus was acquired from Sigma (Catalog #: P7854). The mAb Myc-Tag (71D10) was purchased from Cell Signaling (Catalog #: 2278). The β-actin antibody or GAPDH was purchased from Sigma and used as an internal protein control. The Alexa Fluor 488 and Cy3 conjugated secondary antibodies were purchased from ThermoScientific and Jackson ImmunoResearch, respectively. The HRP-conjugated secondary antibodies (anti-mouse and anti-rabbit) were purchased from Pierce and previously reported. The dilution factor for primary and secondary antibodies was 1: 1000 and 1: 10,000, respectively.

2.6. Cell Lysis and Protein Amount Quantification

Cell conditioned medium and lysates were prepared using previously reported methods (Ward et al., 2017; Zhang et al., 2010a, 2007). Briefly cells were lysed in M-PER (Mammalian Protein Extraction Reagent, Thermoscientific) with 1× Halt protease inhibitor cocktail (Thermoscientific). The lysates were collected, centrifuged at 10,000 *g* for 20 min, pellets were discarded, and supernatants were transferred to a new Eppendorf tube. Total protein was quantified using the BCA protein assay kit (Pierce).

2.7. Western Blotting Analysis (WB)

WB analysis was carried out by the method previously described (Ward et al., 2017; Zhang et al., 2010a, b). Briefly, proteins were extracted and applied to electrophoresis using the Novex NuPAGE SDS-PAGE Gel System (Thermo Fisher Scientific), followed by membrane transfer, antibody incubation, and signal development. The house-keeping protein, β-actin or GAPDH, was used as an internal control. The VersaDoc imaging system with Quantity One software (Bio-Rad) and the Odyssey® Fc with Image Studio imaging software (LI-COR) were used to develop the blots and quantify the proteins of interest following protocols previously described (Ward et al., 2017; Zhang et al., 2010a, b). ImageJ was also used for the analyzing of blots.

2.8. Aβ Measurements

Aβ measurements were performed following the previously-reported protocols and as suggested by the manufacturers, including Wako (Zhang et al., 2010a, 2010b) and MSD MesoScale Diagnostics (Kounnas et al., 2010). In brief, Aβ40 and Aβ42 levels were quantified using a sandwich enzyme-linked immunosorbent assay (ELISA) from Wako. The MSD triplex (Aβ40, Aβ38 and Aβ42) were measured via an electrochemiluminescence-based multi-array method to validate the results observed for the ELISA (Wako). Aβ levels from samples treated with GSMs or GSIs were compared and normalized to those levels of vehicle control treatment.

2.9. Immunocytochemistry

The methods for immunocytochemistry were previously reported (Uemura et al., 2011; Zoltowska et al., 2017). Briefly, cells were fixed by 15-minute incubation with 4% paraformaldehyde (PFA) in phosphate buffered saline (PBS) and then washed with PBS and permeabilized with 0.1% Triton-× 100 in PBS. The non-specific binding of the antibodies in the samples was blocked by 1.5% normal donkey serum (NDS) (Jackson ImmunoResearch Labs, West Grove, PA) in PBS for 1 h. The cells were then incubated overnight at 4 °C with respective primary antibodies: mouse anti-PS1 N-terminus and rabbit anti-PS1 loop or PS1 CT antibodies diluted in PBS supplemented with 1.5% NDS. This was followed by 1-h incubation with corresponding Alexa Fluor 488- and Cy3-conjugated secondary antibodies. Vectashield mounting medium was used to mount the slides (Vector Laboratories, Inc., Burlingame, CA), which was subsequently applied to PS1 conformation analysis via FLIM.

2.10. Fluorescence Lifetime Imaging Microscopy (FLIM) Analysis

PS1 conformation was analyzed using previously established Förster resonance energy transfer (FRET)-based FLIM analysis (Maesako et al., 2017; Uemura et al., 2009; Zoltowska et al., 2017), which allows determination of the proximity between PS1 subdomains, e.g. the N-terminus (NT) and C-terminus (CT) or the cytoplasmic loop domain. Briefly, the CHO cells were stained with the primary antibodies specific for various PS1 subdomains, and then Alexa Fluor 488 (AF488) and Cy3-labeled secondary antibodies were used as the donor and acceptor fluorophores, respectively. AF488 fluorophore (two-photon excitation at 780 nm wavelength) was excited using pulsing Chameleon Ti:Sapphire laser (Coherent Inc., Santa Clara, CA). The donor fluorophore lifetimes were recorded using a high-speed photomultiplier tube (MCP R3809; Hamamatsu, Bridgewater, NJ) and a fast time-correlated single-photon counting acquisition board (SPC-830; Becker & Hickl, Berlin, Germany). When the acceptor is present close to the donor, the transfer of the donor emission energy (FRET) to the acceptor occurs, resulting in the shortening of the donor fluorophore lifetime (τ2). Samples, where the anti-PS1 loop CT antibody was omitted, were used as a negative control to determine the baseline lifetime of the donor fluorophore

labelling PS1 NT (AF488) (τ1). The percent FRET efficiency ($E_{FRET\%}$) is calculated using the following equation: $E_{FRET\%} = (\tau 1 - \tau 2)$ divided by $\tau 1 * 100\%$. The data were analyzed using SPC Image software (Becker & Hickl, Berlin, Germany).

2.11. Data Analysis

β-Actin was used in the Western blotting analysis to account for any differences in loading. The levels of various proteins, e.g. full length APP, C99, and C83 were normalized to the β-actin values from the same lane or sample. All results were demonstrated as means ± S.E. from at least three experiments. We used the two-tailed Student's t-test or one-way analysis of variance (ANOVA), as appropriate, to reveal the differences between the experimental groups. P values <0.05 were considered statistically significant.

3. Results

3.1. SGSM-36 Preferentially Decreases Aβ42 Levels in Tg2576 Mice

The Tg2576 mouse model is a well-characterized model for studying AD in which mice overexpress the EOFAD-linked Swedish mutation-containing form of APP that increases total Aβ levels (Hsiao et al., 1996). Prior experiments have demonstrated that acute administration of the parent 2-aminothiazole GSM effectively reduced brain and plasma Aβ42 levels in Tg2576 mice (Kounnas et al., 2010). Consequentially, experiments were designed which investigate whether acute treatment with SGSM-36 (Fig. 1A), a small molecule compound with improved physicochemical properties, would also reduce Aβ42 levels in the brain and plasma of Tg2576 mice (Kounnas et al., 2010). Following a previously-established protocol,

Tg2576 mice were treated with vehicle or 25 mg/kg SGSM-36 once daily for three consecutive days (Kounnas et al., 2010). Upon completion of the study, the brains were harvested 3 h after last dose and then processed to generate a TBS soluble fraction and a TBS insoluble fraction. The TBS insoluble samples were further processed in 70% formic acid to generate TFA sample fractions. Subsequently, the Meso Scale Aβ triplex assay was carried out to the detect Aβ levels (Aβ38, Aβ40 and Aβ42) in the processed samples.

Aβ40 and Aβ42 were both detected within the samples; however, Aβ38 was not detected due to the low levels of this peptide, consistent with other AD transgenic models (Minter et al., 2016). Treatment with SGSM-36 did not significantly change Aβ40 or Aβ42 levels compared to vehicle for the TBS-soluble fractions (Fig. 1B). The raw values of Aβ levels were also represented (Supplementary Fig. 1). A 30.5% decrease in Aβ42 levels in the soluble fraction was associated with acute treatment, although the difference was below the statistical significance level using ANOVA ($p > 0.05$). The levels of Aβ40 in the TBS-insoluble fractions were suppressed by 26.9% when compared to vehicle, which did not reach the statistical significance level ($p > 0.05$). Importantly, SGSM-36 treatment led to a significant decrease in Aβ42 levels (42.0% reduction) in TBS-insoluble brain samples ($p < 0.05$) (Fig. 1C).

Furthermore, the effects of SGSM-36 on plasma Aβ levels were determined. As in the brain soluble fraction, little differences in plasma Aβ40 levels were observed between SGSM-36 and vehicle treated groups. However, SGSM-36 decreased plasma Aβ42 levels by 46.2% compared to vehicle ($p < 0.01$) (Fig. 1D), which resulted in a substantial reduction of the Aβ42: Aβ40 ratio in plasma (41.1% decrease) as compared to control ($p < 0.05$) (Fig. 1E). Analysis of brain Aβ (42:40) ratios, which drives the β-amyloid burden, found that acute treatment with SGSM-36 decreased Aβ (42:40) ratios in both brain soluble and
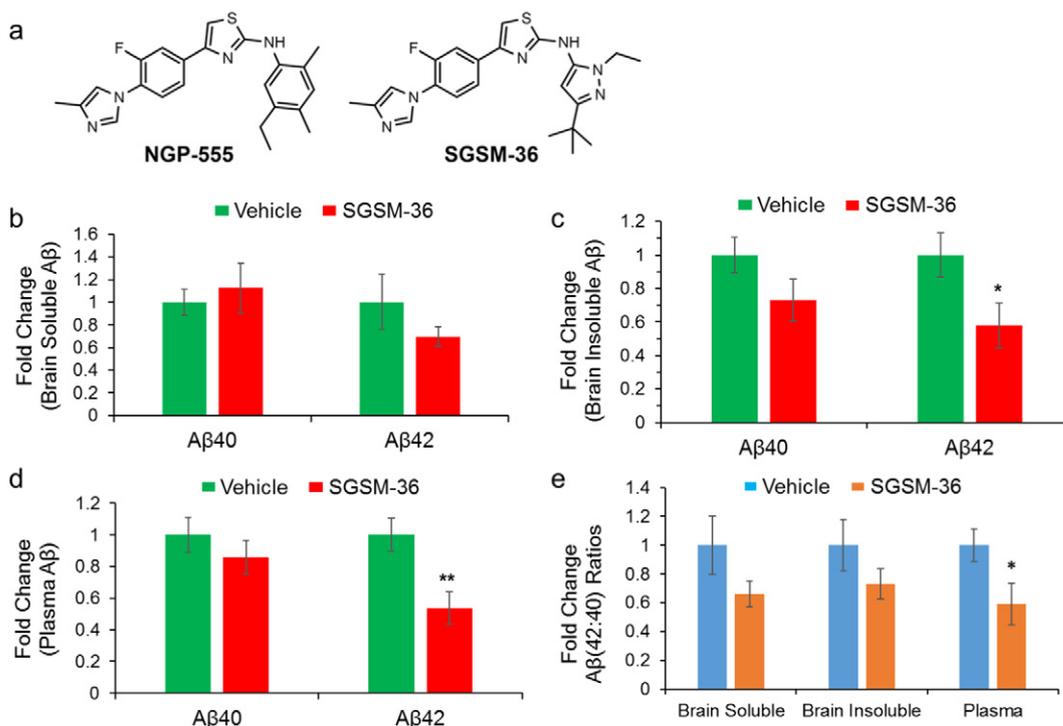

Fig. 1. Aminothiazole-derived compound SGSM-36 was designed based on parent compound, and preferentially decreased Aβ42 levels and changed the Aβ (42:40) ratios in Tg2576 mice. The parent aminothiazole compound, NGP-555, was optimized for improved properties, which led to generation of aminothiazole-derived compound SGSM-36 (A). SGSM-36 was applied to an AD transgenic animal-based efficacy study for Aβ42 inhibition (B–D). Three-month old female Tg2576 mice were treated with vehicle (80% PEG-400 v/v; n = 8) or 25 mg/kg SGSM-36 (n = 7) for 3 consecutive days. Mouse brains were processed to generate TBS-soluble and TBS-insoluble solutions. Brain samples and plasma were then applied to MesoScale Aβ analysis to determine Aβ levels and Aβ (42:40) ratios. A. Structures of aminothiazole-based parent compound NGP-555 and SGSM-36. B. SGSM-36 did not significantly decrease brain TBS-soluble Aβ40 and Aβ42 levels compared to vehicle ($p > 0.05$). C. SGSM-36 significantly decreased brain TBS-insoluble Aβ42 levels versus vehicle ($p < 0.05$). D. SGSM-36 significantly decreased plasma Aβ42 levels compared to vehicle ($p < 0.05$). E. SGSM-36 decreased Aβ (42:40) ratios in brain TBS-insoluble portion and plasma. Mean ± S.E.; ANOVA; *$p < 0.05$; **$p < 0.01$.

insoluble samples by 34.0% and 26.8%, respectively, which however were below the statistical significance level (p values > 0.05; Fig. 1E). Collectively, our data show that SGSM-36 preferentially decreases brain and plasma Aβ42 levels in Tg2576 mice. These results are consistent with the effects of the parent 2-aminothiazole GSM in these mice (Kounnas et al., 2010).

3.2. SGSM-36 Does Not Affect α or β-secretase Processing of APP in Tg2576 Mice

To expand upon prior research and gain insights with respect to the effects of SGSM-36 on APP processing, Western blot analysis of mouse brains treated with SGSM-36 or vehicle was performed. Measurement
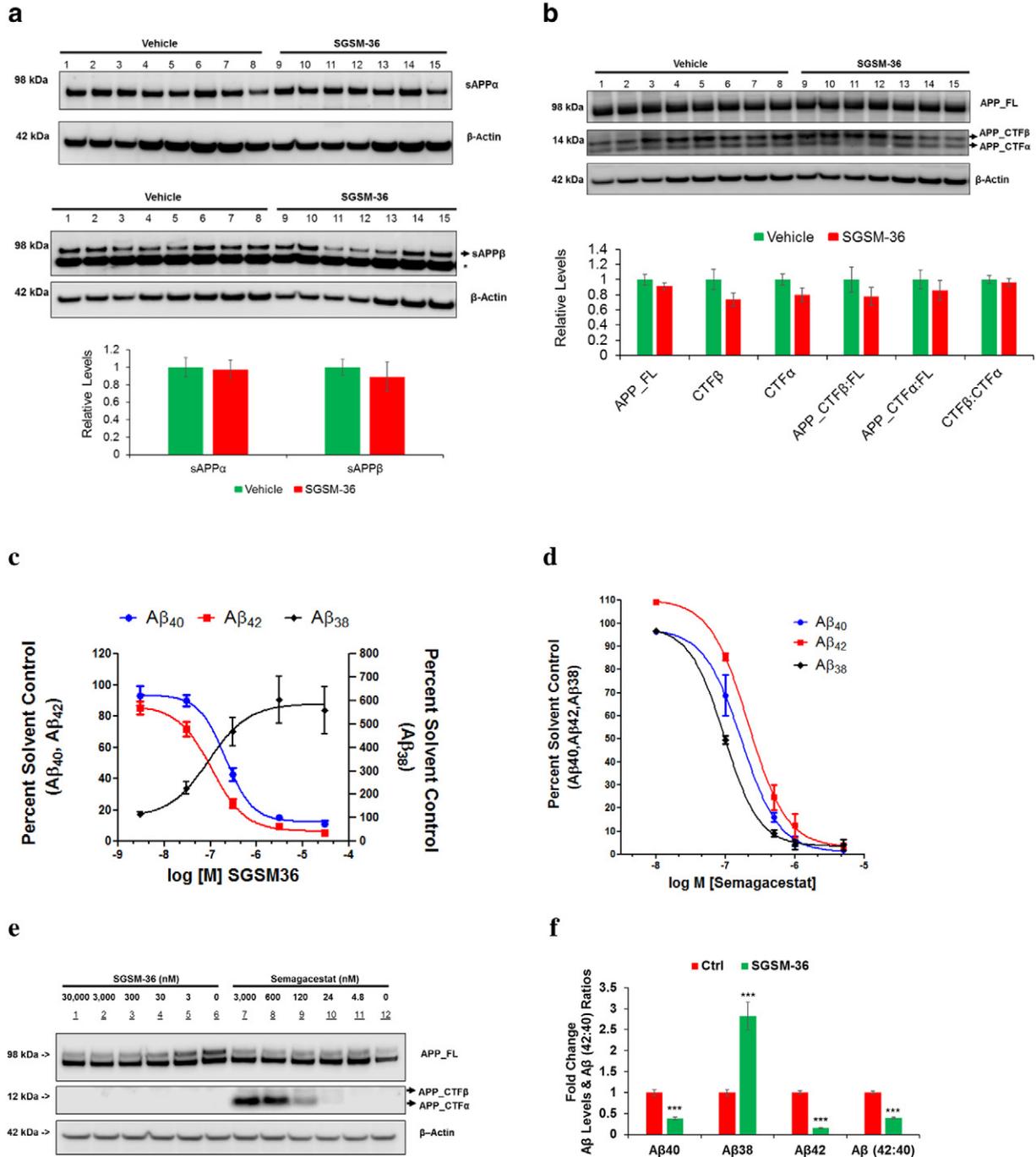

Fig. 2. SGSM-36 did not significantly affect APP processing via α-, or β-secretase in AD mouse brains and cells with FAD mutations. A. sAPPα and sAPPβ proteins were detected through Western blotting analysis (via 6E10 and sAPPβ antibody, respectively) using mouse brain TBS-soluble samples. Additionally, a house-keeping protein, β-actin was used as the control for normalization of proteins of interest. Bottom row is the densitometric quantification of WB. n = 8 (vehicle) and n = 7 (SGSM-36). B. APP full length and proteolytic fragments (APP_FL and CTFα or β) were analyzed in mouse brain MTBS samples by WB using the G12A antibody. Bottom row is the densitometric quantification of WB. Bottom row is the densitometric quantification. n = 8 (vehicle) and n = 7 (SGSM-36). C–D. SGSM-36 preferentially decreased Aβ42 levels (C), unlike semagacestat (a GSI) which decreased the levels of all Aβ species (D). APP[Indiana]-expressing 7PA2 cells were treated with different doses of semagacestat or SGSM-36 for up to 24 h. Medium was applied to Aβ-MSD to detect the levels of Aβ (40,38,42). E. SGSM-36 did not change the levels of APP-CTFs, unlike semagacestat which increased APP-CTFs. 7PA2 cells were treated with different doses of semagacestat or SGSM-36 for up to 24 h. Lysates were applied to WB to detect full length APP and APP-CTFs via the G12A antibody. β-Actin was used as the loading control. F. SGSM-36 preferentially decreased the levels of Aβ42 over Aβ40, while increased Aβ38 levels in 3D–differentiated FAD HReN cells. The FAD HReN cells expressing APP Swedish and London mutations and PSEN1 δE9 mutation were 3D–differentially for 5 weeks and then treated with 400 nM SGSM-36 or DMSO for another 2 weeks. Medium were applied to Aβ-MSD to calculate Aβ levels. n = 5; Mean ± S.E.; ANOVA; ***p < 0.001.

of sAPPα (via 6E10 antibody) and sAPPβ (via sAPPβ antibody) in the TBS-soluble fraction revealed that there was no statistically significant impact upon α or β-secretase processing of APP when comparing vehicle and SGSM-36 treatment (p > 0.05) (Fig. 2A). Particularly, we observed that SGSM-36 decreased the levels of sAPPβ by 10.8% compared to control (p > 0.05).

As a means to interrogate target specificity, membrane protein-containing, or MTBS portions, were utilized to detect full length APP (APP-FL) and APP-CTFs via G12A, a previously reported antibody targeting APP-CTFs (Griciuc et al., 2013; Wang et al., 2015). As anticipated, SGSM-36 did not affect the levels of full length APP (Fig. 2B). Additionally, SGSM-36 did not alter the levels of APP-CTFβ or APP-CTFα, the cleavage products of BACE-1 and α-secretase, respectively (Fig. 2B). Specifically, SGSM-36 decreased the levels of APP-CTFα and APP-CTFβ by 26.08% and 20.48%, respectively, compared to control (p values > 0.05). As a result of the mode of action and target selectivity exhibited by SGSM-36, compound treatment did not increase the levels of APP proteolytic processing products via α or β-secretase as observed with conventional GSIs.

3.3. SGSM-36 Preferentially Decreases $A\beta_{42}$ Levels in Cells Expressing FAD Mutations, but Not Semagacestat

In order to further explore the potential of this compound, Aβ levels were measured in cells with an alternative FAD mutation in APP following treatment with SGSM-36, semagacestat, or vehicle. A CHO cell line stably expressing human APP751 bearing the V717F Indiana mutation (also known as 7PA2 cells) (Welzel et al., 2014), which expresses >10-fold higher levels of Aβ40 and Aβ42 compared to CHO-APP751 cells (Zhang et al., 2010c), was treated with SGSM-36 at concentrations of 0, 3, 30, 300, 3000, and 30,000 nM for 24 h. Collection of the medium showed that SGSM-36 decreased both Aβ40 and Aβ42 levels, while simultaneously increasing Aβ38 levels. Consistent with prior report using SH-SY5Y cells stably overexpressing human APP751 (Wagner et al., 2014), the IC_{50} values for Aβ40 and Aβ42 in medium were 214.50 nM and 106.10 nM, respectively, and the EC_{50} value for Aβ38 levels in medium was 90.94 nM (Fig. 2C). Conversely, 7PA2 cells treated with semagacestat (0, 4.8, 24, 120, 600, and 3000 nM) for 24 h showed decreases in all Aβ species measured from medium with IC_{50} values of 21.69 nM, 38.25 nM, and 46.66 nM for Aβ38, Aβ40, and Aβ42 respectively (Fig. 2D).

In addition, the impact of treatment with SGSM-36 or semagacestat upon γ-secretase processing of APP was determined by WB analysis utilizing the G12A antibody to assess full length APP and APP-CTFs levels. Incubation with semagacestat up-regulated the levels of APP-CTFs in addition to a less pronounced increase in full length APP, while SGSM-36 did not affect the APP-CTFs or full length APP levels in 7PA2 cells (Fig. 2E). Furthermore, the 3D human neural cell culture expressing APP Swedish and London mutations and PSEN1 δE9 mutation, also known as HReN-mGAP cells were utilized to validate the roles of SGSM-36 on Aβ levels. These cells were 3D-differentially for 5 weeks and then treated with 400 nM SGSM-36 or DMSO for another 2 weeks. SGSM-36 led to a significant decrease in Aβ40 and Aβ42 level by 61.8% and 84.9%, respectively, as well as an increase in Aβ38 by 182.5%, compared to control (n = 5; ANOVA; p values < 0.001) (Fig. 2F). Notably, SGSM-36 significantly decreased Aβ (42:40) ratios by 60.4% compared to control (p < 0.001) (Fig. 2F). The raw values of Aβ levels were also represented (Supplementary Fig. 2). Collectively, SGSM-36 preferentially decreased Aβ42 levels in AD transgenic mice and various model cells with FAD mutations in APP without affecting α- or β-secretase processing of APP.

3.4. SGSM-36 Does Not Affect Notch Processing in Tg2576 Mice and Cells Expressing FAD Mutations

Next, the effect of treatment with SGSMs versus GSIs on Notch processing, an essential event during development, was compared (Kopan et al., 1994). Mouse brain MTBS samples were examined by WB using the monoclonal Notch1 antibody. Consistent with the results of other SGSMs using cell-based models, treatment with SGSM-36 did not influence the levels of cleaved Notch1 protein (Notch1-CTF), as compared to vehicle (p > 0.05) (Fig. 3A). In addition, the effects of SGSM-36 on Notch processing were further validated using APP^Indiana-expressing 7PA2 cells, as compared to semagacestat. 7PA2 cells were transfected with the NδED construct and then treated with different doses SGSM-36 (up to 20,000 nM) or semagacestat (up to 2000 nM) for 24 h. Cell lysates were applied to WB and Myc antibody was utilized to assess the NδED and NICD tagged with Myc on their C-termini. SGSM-36 treatment did not change the NICD levels at any concentration studied, while semagacestat decreased NICD levels even at low concentrations (Fig. 3B). Collectively, these experiments demonstrate that this class of SGSMs reliably utilizes a mechanism of action which modulates γ-secretase resulting in preferentially decreasing Aβ42 levels while not affecting the enzyme's processing of Notch.

3.5. SGSM-36 Modulates PS1 Conformational Change

Next, we investigated the potential roles of SGSM-36 on PS1 conformational changes using a fluorescence lifetime imaging microcopy (FLIM) assay, which have been well-established to reliably monitor changes in Aβ (42:40) ratios (Uemura et al., 2010, 2009). Specifically, the FRET efficiencies between the fluorophores labelling PS1 N-terminus and loop domain in CHO-APP751 cells transfected with the GFP-PS1-RFP FRET reporter probe (Uemura et al., 2009) (Fig. 4A), as well as mouse primary neurons immunostained with fluorescently labeled antibodies against endogenous PS1 N- and C-termini were assessed (Fig. 4B). The cells were pre-treated for 16 h with SGSM-36 or vehicle control and the FRET efficiency was subsequently reported for outlined whole-cell and cell periphery of CHO-APP751 cells transfected with GFP-PS1-RFP FRET reporter (Fig. 4A), and for cell bodies and processes of mouse primary neurons expressing PS1 at endogenous levels (Fig. 4A). The average FRET efficiency between the fluorophores labelling the PS1 subdomains after SGSM-36 treatment was reduced in both CHO-APP751 and primary neurons, as compared to the vehicle controls (Fig. 4A–B). The decrease was most profound at the periphery of the CHO cells and in the neuronal processes, which represent the membrane-enriched structures. The consistent reduction of the FRET efficiency in both SGSM-36 treated cell types indicates the decrease in the proximity between the PS1 NT and CT loop domains, reflective of the predominantly "open" non-pathogenic PS1 subdomain arrangement. Collectively, the FLIM-based PS1 conformational analyses provide further mechanistic insight into how SGSMs decrease Aβ (42:40) ratios.

4. Discussion

Although AD is a genetically complex disease, 225 known familial AD (FAD) mutations in PSEN1 and PSEN2 afford direct evidence for the importance of PS1 and γ-secretase with respect to the disorder. In addition, most of the 51 FAD mutations in APP are also characterized by altered biological activity of γ-secretase directly affecting the type of Aβ species produced. Biochemical studies of these mutations show a common endpoint which is primarily characterized by increases in the levels of Aβ42 and the Aβ (42:40) ratios, driving the aggregation of Aβ into neurotoxic oligomeric assemblies (Bertram and Tanzi, 2008; Tanzi and Bertram, 2005). Therefore, elucidating the physiological and pathophysiological roles of γ-secretase, and its cleavage products, (e.g. Aβ) are key to evaluating the therapeutic potential of this target for the treatment of AD.

The strong implication based on the genetics of AD that the constitution of the Aβ fragments is a central cause of AD led to γ-secretase emerging as a prime therapeutic target. Initially, GSI's garnered intense interest based on their ability to reduce the levels of all Aβ species through a broad-based inhibitory mechanism. However, inhibition of
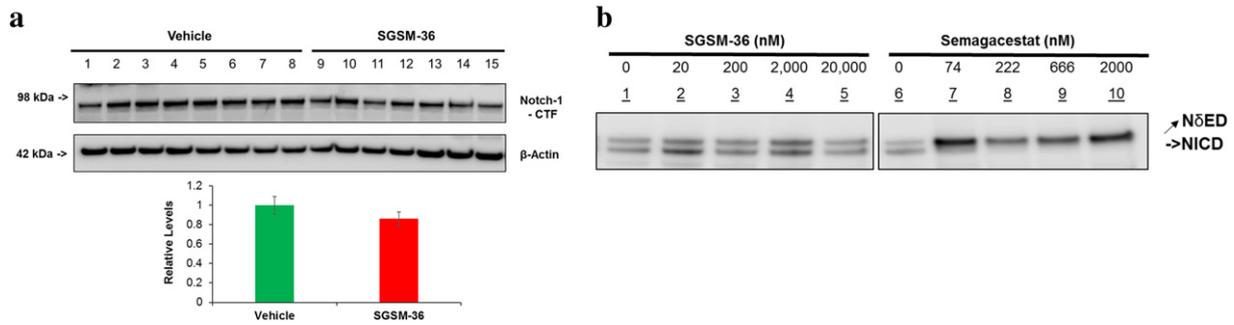
Fig. 3. SGSM-36 did not change proteolytic processing of Notch, while semagacestat inhibited Notch processing. A. SGSM-36 did not change Notch processing in Tg2576 mice brains compared to vehicle. SGSM-36 or vehicle-treated mouse brain MTBS proteins were applied to WB and detected by the Notch antibody. Bottom row is the densitometric quantification. n = 8 (vehicle) and n = 7 (SGSM-36). B. SGSM-36 did not inhibit Notch processing, while semagacestat down-regulated Notch processing in APP^{Indiana}-expressing 7PA2 cells. 7PA2 cells were transfected with the NδED construct and then treated with different doses SGSM-36 or semagacestat for additional 24 h. Cells were harvested 48 h post transfection and applied to WB. Myc antibody was utilized to assess the NδED and NICD tagged with Myc on their C-termini. SGSM-36 did not inhibit Notch processing at all concentrations tested, while semagacestat inhibited Notch processing.

the γ-secretase enzyme led to unanticipated consequences; GSI treatment arrested the proteolytic processing of alternative γ-secretase substrates including Notch leading to significant adverse events. Additionally, inhibiting the processing of APP resulted in the accumulation of upstream CTFs, particularly APP-CTFβ, which is responsible for initiating neurodegenerative process and cognitive decline (Lauritzen et al., 2012). The failure of GSIs as a therapy for AD fueled intense scrutiny of γ-secretase as a target and led to various studies in the genetics, biochemistry and pharmacology to determine the biological roles and numerous substrates of the enzyme.

Despite the stigma attached to targeting γ-secretase engendered by GSI's, an alternative class of small molecules, known as GSMs, has been developed, which bind to an allosteric site within the enzyme (Uemura et al., 2010, 2009) and modulate the Aβ isoforms produced. Specifically, GSM treatment attenuates the production of the longer, more fibrillogenic Aβ42 peptide in favor of shorter and more soluble species (i.e. Aβ37 and Aβ38). Since GSMs do not interfere with γ-secretase function, these compounds are likely avoiding the adverse events of GSI's. The clear mechanistic differentiation of GSIs and GSMs is paramount to the development of GSMs for the treatment and prevention of AD. To this end, a thorough investigation of the molecular endo-phenotypes using both cell- and animal-based models of AD, comparing a conventional GSI and a SGSM currently under development has been described in the current study.

During the course of the development of aminothiazole-derived small molecule GSMs, SGSM-36 (Fig. 1A) was discovered and exhibited

good activity for suppressing the production of Aβ42 (Aβ42 IC50 = 63 nM) (Rynearson et al., 2016; Wagner et al., 2014). In addition, SGSM-36 exhibited improved physicochemical properties with respect to the parent compound including good aqueous solubility, as well as acceptable in vivo pharmacokinetic behavior in mice (Wagner et al., 2014). In order to build upon prior studies, a thorough in vivo efficacy analysis of SGSM-36 using Tg2576 mice showed that treatment at 25 mg per kg for 3 consecutive days was effective at reducing brain (Fig. 1B–C) and plasma (Fig. 1D) Aβ42 levels and Aβ (42:40) ratios in both brain and plasma (Fig. 1E). In comparison to the parent compound NGP-555 (or compound-4) (Kounnas et al., 2010), a nearly 2-fold superior decrease in brain Aβ42 levels was achieved following treatment with SGSM-36, although there is a greater than six-fold disparity between the in vitro Aβ42 IC$_{50}$ values of the parent compound and SGSM-36 (Kounnas et al., 2010; Wagner et al., 2014). Furthermore, the parent compound NGP-555 was 2-fold superior to SGSM-36 for reducing plasma Aβ42 levels, suggesting that the highly lipophilic nature of this compound is resulting in sequestration of the drug in the periphery which likely associated with high plasma protein binding thereby limiting the effect in the brain. Additionally, the efficacy data belies the brain to plasma ratio of the parent compound and SGSM-36 (brain:plasma = 0.93 and 0.54, respectively), demonstrating that the ratio can be a valuable tool to assess whether a compound can cross the blood-brain barrier but is unlikely to accurately capture the in vivo activity of a given compound. Based on the efficacy data, SGSM-36 exhibits good therapeutic potential, since the overall goal of treatment is to reduce Aβ42 in the brain. Furthermore, SGSM-36 clearly
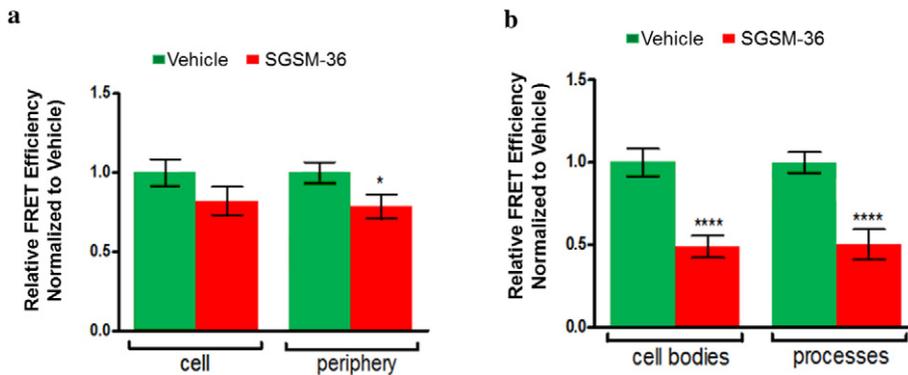

Fig. 4. SGSM-36 modulates conformation of PS1. SGSM-36 led to reductions in the FRET efficiency, indicative of the "open" PS1 conformation, in both CHO-APP751 cells (A) and primary mouse neurons (B). A. CHO-APP751 cells transfected with GFP-PS1-RFP were treated with vehicle or 500 nM SGSM-36 for 16 h. The PS1 conformation was analyzed by FLIM via monitoring the GFP and RFP proximity on PS1 NT and transmembrane 6–7 loop domains, respectively. Reduction in the FRET efficiency was recorded upon SGSM-36 treatment and compared to vehicle. Mean ± S.E.; n = 30–40 from 3 independent experiments. B. Primary mouse neurons were treated with vehicle or 200 nM SGSM-36, for 16 h and then applied to antibody-based FLIM assay to monitor conformational changes in endogenous PS1. Reduction in the FRET efficiency was recorded in neurons upon SGSM-36 treatment compared to vehicle. Mean ± S.E.; n = 35–81 neurons from 3 independent experiments. Two-tailed unpaired Student's t-test, *p < 0.05; ****p < 0.0001.

demonstrates that strategies which account for physicochemical properties can be applied to the identification analogs with improved potential.

To address target specificity in vivo, samples from Tg2576 mouse brains and cell lysates transfected with Notch constructs were subjected to western blot analysis. Distinct from GSIs, SGSM-36 did not affect the levels of cleaved Notch1 protein in mouse brains (Fig. 3A) and NICD levels in cells (Fig. 3A) indicating a unique mechanism of action that does not interfere with γ-secretase, thereby precluding inhibition related side-effects. Moreover, detection of upstream cleavage products, sAPPα and sAPPβ, shows that SGSM-36 does not impact enzymatic processing of APP by BACE-1 or α-secretase, indicating that the observed shift in the Aβ profile results from modulation of the γ-secretase enzyme (Fig. 2A and B).

A comparison of the mode of action of SGSM-36 and semagacestat, a GSI, was also conducted using a CHO cell line stably expressing human APP751 bearing the V717F Indiana mutation. Although the sequence of APP is distinct from the aforementioned in vivo study, SGSM-36 treatment resulted in dose-dependent decreases in Aβ42 and Aβ40, as well as a dose-dependent increase Aβ38, whereas reduction of all three Aβ analyzed was associated with semagacestat treatment (Fig. 2C and D). Consistent with discrete mechanisms of action, SGSM-36 modulates the constitution of the Aβ peptide profile, while semagacestat inhibits enzyme function. Analysis of APP-CTFs further supports the observed activities. SGSM-36 did not influence the levels APP-CTFs; however, the GSI, semagacestat showed dose-dependent accumulation of the γ-secretase substrate (Fig. 2E). The effects of SGSM-36 on Aβ levels in the CHO cell line were validated in our human 3D–differentiated neural cell culture expressing FAD mutations containing *APP* K670N/M671L (Swedish) and V717I (London) mutations and *PSEN1* δE9 mutation (Fig. 2F). The presented characterization of the mechanisms of these pharmacological agents which target γ-secretase serves to distinguish GSMs from GSIs with respect to their impact upon the biological roles of γ-secretase. By avoiding inhibition of the γ-secretase enzyme, SGSM-36 will avoid instigating the side effects of GSIs while still efficaciously impacting the primary biomarker associated with AD, Aβ42. These studies encourage further evaluation of SGSM-36 toward the development of an amyloid directed therapy. The results of this study also warrant investigation of the roles of SGSM-36 on other γ-secretase related activity and proteins, e.g. AICD protein.

GSIs were shown to effectively decrease Aβ levels at doses close to or higher than their IC$_{50}$ values in cell culture models. Surprisingly, they also slightly increase Aβ levels at low doses, (significantly below the IC$_{50}$) also known as "Aβ rise", due to various mechanisms including inhibition of cellular γ-secretase activity (Barnwell et al., 2014; Burton et al., 2008; Citron et al., 1996; Lanz et al., 2006; Mitani et al., 2012). Particularly, a potent peptidomimetic GSI, semagacestat, increases Aβ42 levels at low doses in H4 cells stably over-expressing an FAD-linked Swedish double mutation and also increases Aβ42 levels in CSF and plasma of treated guinea pigs. These preclinical outcomes recapitulate the biomarker results of semagacestat's clinical trials for AD (Fleisher et al., 2008).

Previous studies have shown that PS1 exists in a dynamic equilibrium of different conformational states, characterized by varied proximities between the PS1 NT and CT large cytosolic loop domain (Kuzuya et al., 2016; Maesako et al., 2017; Uemura et al., 2010). Importantly, PS1 subdomain arrangement strongly correlates with the changes in Aβ (42:40) ratios (Kuzuya et al., 2016; Maesako et al., 2017; Uemura et al., 2010; Zoltowska et al., 2017). For example, fenofibrate, an antilipidemic agent that potently increases the Aβ (42:40) ratios (Kukar et al., 2005) leads to shortening of the donor fluorophore lifetime (τ1) and increased FRET efficiency, which indicates a closer proximity of PS1 subdomains, or 'closing' of PS1 conformation (Uemura et al., 2010). Alternatively, ibuprofen, a small molecule that belongs to the group of nonsteroidal anti-inflammatory drugs (NSAIDs) known to decrease the Aβ (42:40) ratios results in "opening" of PS1

conformation (Uemura et al., 2010). Taken together, a pharmacological agent that elicits an "opening" of PS1 conformation should preferentially decrease relative levels of the longer, Aβ42 species and may have potential as a treatment for AD. Consistent with the in vitro and in vivo results showing attenuation of Aβ42, the antibody-based FLIM PS1 conformation assay demonstrate that SGSM-36 induces a conformational shift within the endogenous PS1 molecule toward the "open", non-pathogenic state (Fig. 4A and B). The FRET data points toward a potential molecular mechanism in which SGSM-36 reduces Aβ (42:40) ratios by instigating a shift in the structure of the enzyme resulting in enhanced proteolytic processing of the substrate.

In summary, acute treatment with SGSM-36 led to significant reduction in plasma and brain Aβ42 levels in Tg2576 mice. Thorough scrutiny of the in vivo and in vitro mechanism of action studies demonstrate that SGSM-36 suppresses the formation of Aβ42 through the modulation of the γ-secretase enzyme in a fashion distinct from previously developed GSIs. Collectively, these results indicate that using SGSMs are a superior therapeutic approach for addressing amyloid when compared to conventional GSIs. The good in vivo efficacy observed for SGSM-36 warrants further study toward the development of an effective therapy for the treatment and prevention of AD.

Conflicts of Interest

None.

Author Contributions

C.Z., R.E.T and S.L.W. performed experimental design and data interpretation. F.R., J. F. W., K.M.Z., Y·W, S.H.C., S.J.M., X.S. and C.Z. conducted the experiments. F.R., J.F.W., K.D.R. O.B., R.E.T. and C.Z. contributed to writing and revising the manuscript. K.D.R. and S.L.W. prepared SGSMs and revised the manuscript.

Appendix A. Supplementary Data

Supplementary data to this article can be found online at https://doi.org/10.1016/j.ebiom.2017.08.028.

References

Barnwell, E., Padmaraju, V., Baranello, R., Pacheco-Quinto, J., Crosson, C., Ablonczy, Z., Eckman, E., Eckman, C.B., Ramakrishnan, V., Greig, N.H., et al., 2014. Evidence of a novel mechanism for partial gamma-secretase inhibition induced paradoxical increase in secreted amyloid beta protein. PLoS One 9, e91531.

Berezovska, O., Frosch, M., McLean, P., Knowles, R., Koo, E., Kang, D., Shen, J., Lu, F.M., Lux, S.E., Tonegawa, S., et al., 1999. The Alzheimer-related gene presenilin 1 facilitates notch 1 in primary mammalian neurons. Brain Res. Mol. Brain Res. 69, 273–280.

Bertram, L., Tanzi, R.E., 2008. Thirty years of Alzheimer's disease genetics: the implications of systematic meta-analyses. Nat. Rev. 9, 768–778.

Brendel, M., Jaworska, A., Herms, J., Trambauer, J., Rotzer, C., Gildehaus, F.J., Carlsen, J., Cumming, P., Bylund, J., Luebbers, T., et al., 2015. Amyloid-PET predicts inhibition of de novo plaque formation upon chronic gamma-secretase modulator treatment. Mol. Psychiatry 20, 1179–1187.

Burton, C.R., Meredith, J.E., Barten, D.M., Goldstein, M.E., Krause, C.M., Kieras, C.J., Sisk, L., Iben, L.G., Polson, C., Thompson, M.W., et al., 2008. The amyloid-beta rise and

gamma-secretase inhibitor potency depend on the level of substrate expression. J. Biol. Chem. 283, 22992–23003.

Choi, S.H., Kim, Y.H., Hebisch, M., Sliwinski, C., Lee, S., D'Avanzo, C., Chen, H., Hooli, B., Asselin, C., Muffat, J., et al., 2014. A three-dimensional human neural cell culture model of Alzheimer's disease. Nature 515, 274–278.

Citron, M., Diehl, T.S., Gordon, G., Biere, A.L., Seubert, P., Selkoe, D.J., 1996. Evidence that the 42- and 40-amino acid forms of amyloid beta protein are generated from the beta-amyloid precursor protein by different protease activities. Proc. Natl. Acad. Sci. U. S. A. 93, 13170–13175.

D'Avanzo, C., Sliwinski, C., Wagner, S.L., Tanzi, R.E., Kim, D.Y., Kovacs, D.M., 2015. Gamma-secretase modulators reduce endogenous amyloid beta42 levels in human neural progenitor cells without altering neuronal differentiation. FASEB J. 29, 3335–3341.

De Strooper, B., 2014. Lessons from a failed gamma-secretase Alzheimer trial. Cell 159, 721–726.

Doody, R.S., Raman, R., Farlow, M., Iwatsubo, T., Vellas, B., Joffe, S., Kieburtz, K., He, F., Sun, X., Thomas, R.G., et al., 2013. A phase 3 trial of semagacestat for treatment of Alzheimer's disease. N. Engl. J. Med. 369, 341–350.

Edbauer, D., Winkler, E., Regula, J.T., Pesold, B., Steiner, H., Haass, C., 2003. Reconstitution of gamma-secretase activity. Nat. Cell Biol. 5, 486–488.

Fleisher, A.S., Raman, R., Siemers, E.R., Becerra, L., Clark, C.M., Dean, R.A., Farlow, M.R., Galvin, J.E., Peskind, E.R., Quinn, J.F., et al., 2008. Phase 2 safety trial targeting amyloid beta production with a gamma-secretase inhibitor in Alzheimer disease. Arch. Neurol. 65, 1031–1038.

Gandy, S., 2005. The role of cerebral amyloid beta accumulation in common forms of Alzheimer disease. J. Clin. Invest. 115, 1121–1129.

Griciuc, A., Serrano-Pozo, A., Parrado, A.R., Lesinski, A.N., Asselin, C.N., Mullin, K., Hooli, B., Choi, S.H., Hyman, B.T., Tanzi, R.E., 2013. Alzheimer's Disease risk gene CD33 inhibits microglial uptake of amyloid beta. Neuron 78, 631–643.

Gu, Y., Sanjo, N., Chen, F., Hasegawa, H., Petit, A., Ruan, X., Li, W., Shier, C., Kawarai, T., Schmitt-Ulms, G., et al., 2004. The presenilin proteins are components of multiple membrane-bound complexes that have different biological activities. J. Biol. Chem. 279, 31329–31336.

Hardy, J., Selkoe, D.J., 2002. The amyloid hypothesis of Alzheimer's disease: progress and problems on the road to therapeutics. Science (New York, NY) 297, 353–356.

Herreman, A., Hartmann, D., Annaert, W., Saftig, P., Craessaerts, K., Serneels, L., Umans, L., Schrijvers, V., Checler, F., Vanderstichele, H., et al., 1999. Presenilin 2 deficiency causes a mild pulmonary phenotype and no changes in amyloid precursor protein processing but enhances the embryonic lethal phenotype of presenilin 1 deficiency. Proc. Natl. Acad. Sci. U. S. A. 96, 11872–11877.

Hsiao, K., Chapman, P., Nilsen, S., Eckman, C., Harigaya, Y., Younkin, S., Yang, F., Cole, G., 1996. Correlative memory deficits, Abeta elevation, and amyloid plaques in transgenic mice. Science (New York, NY) 274, 99–102.

Imbimbo, B.P., Del Giudice, E., Colavito, D., D'Arrigo, A., Dalle Carbonare, M., Villetti, G., Facchinetti, F., Volta, R., Pietrini, V., Baroc, M.F., et al., 2007. 1-(3′,4′-Dichloro-2-fluoro[1,1′-biphenyl]-4-yl)-cyclopropanecarboxylic acid (CHF5074), a novel gamma-secretase modulator, reduces brain beta-amyloid pathology in a transgenic mouse model of Alzheimer's disease without causing peripheral toxicity. J. Pharmacol. Exp. Ther. 323, 822–830.

Kopan, R., Ilagan, M.X., 2004. Gamma-secretase: proteasome of the membrane? Nat. Rev. Mol. Cell Biol. 5, 499–504.

Kopan, R., Nye, J.S., Weintraub, H., 1994. The intracellular domain of mouse Notch: a constitutively activated repressor of myogenesis directed at the basic helix-loop-helix region of MyoD. Development (Camb. Engl.) 120, 2385–2396.

Kounnas, M.Z., Danks, A.M., Cheng, S., Tyree, C., Ackerman, E., Zhang, X., Ahn, K., Nguyen, P., Comer, D., Mao, L., et al., 2010. Modulation of gamma-secretase reduces beta-amyloid deposition in a transgenic mouse model of Alzheimer's disease. Neuron 67, 769–780.

Kukar, T., Murphy, M.P., Eriksen, J.L., Sagi, S.A., Weggen, S., Smith, T.E., Ladd, T., Khan, M.A., Kache, R., Beard, J., et al., 2005. Diverse compounds mimic Alzheimer disease-causing mutations by augmenting Abeta42 production. Nat. Med. 11, 545–550.

Kuzuya, A., Zoltowska, K.M., Post, K.L., Arimon, M., Li, X., Svirsky, S., Maesako, M., Muzikansky, A., Gautam, V., Kovacs, D., et al., 2016. Identification of the novel activity-driven interaction between synaptotagmin 1 and presenilin 1 links calcium, synapse, and amyloid beta. BMC Biol. 14, 25.

Lanz, T.A., Karmilowicz, M.J., Wood, K.M., Pozdnyakov, N., Du, P., Piotrowski, M.A., Brown, T.M., Nolan, C.E., Richter, K.E., Finley, J.E., et al., 2006. Concentration-dependent modulation of amyloid-beta in vivo and in vitro using the gamma-secretase inhibitor, LY-450139. J. Pharmacol. Exp. Ther. 319, 924–933.

Lauritzen, I., Pardossi-Piquard, R., Bauer, C., Brigham, E., Abraham, J.D., Ranaldi, S., Fraser, P., St-George-Hyslop, P., Le Thuc, O., Espin, V., et al., 2012. The beta-secretase-derived C-terminal fragment of betaAPP, C99, but not Abeta, is a key contributor to early intraneuronal lesions in triple-transgenic mouse hippocampus. J. Neurosci. 32, 16243–16255a.

Maesako, M., Horlacher, J., Zoltowska, K.M., Kastanenka, K.V., Kara, E., Svirsky, S., Keller, L.J., Li, X., Hyman, B.T., Bacskai, B.J., et al., 2017. Pathogenic PS1 phosphorylation at Ser367. elife 6.

Minter, M.R., Zhang, C., Leone, V., Ringus, D.L., Zhang, X., Oyler-Castrillo, P., Musch, M.W., Liao, F., Ward, J.F., Holtzman, D.M., et al., 2016. Antibiotic-induced perturbations in gut microbial diversity influences neuro-inflammation and amyloidosis in a murine model of Alzheimer's disease. Sci Rep 6, 30028.

Mitani, Y., Yarimizu, J., Saita, K., Uchino, H., Akashiba, H., Shitaka, Y., Ni, K., Matsuoka, N., 2012. Differential effects between gamma-secretase inhibitors and modulators on

cognitive function in amyloid precursor protein-transgenic and nontransgenic mice. J. Neurosci. 32, 2037–2050.

Potter, R., Patterson, B.W., Elbert, D.L., Ovod, V., Kasten, T., Sigurdson, W., Mawuenyega, K., Blazey, T., Goate, A., Chott, R., et al., 2013. Increased in vivo amyloid-beta42 production, exchange, and loss in presenilin mutation carriers. Sci. Transl. Med. 5, 189ra177.

Rogers, K., Felsenstein, K.M., Hrdlicka, L., Tu, Z., Albayya, F., Lee, W., Hopp, S., Miller, M.J., Spaulding, D., Yang, Z., et al., 2012. Modulation of gamma-secretase by EVP-0015962 reduces amyloid deposition and behavioral deficits in Tg2576 mice. Mol. Neurodegener. 7, 61.

Rynearson, K.D., Buckle, R.N., Barnes, K.D., Herr, R.J., Mayhew, N.J., Paquette, W.D., Sakwa, S.A., Nguyen, P.D., Johnson, G., Tanzi, R.E., et al., 2016. Design and synthesis of aminothiazole modulators of the gamma-secretase enzyme. Bioorg. Med. Chem. Lett. 26, 3928–3937.

Selkoe, D.J., 2001. Alzheimer's Disease: genes, proteins, and therapy. Physiol. Rev. 81, 741–766.

Sisodia, S.S., St George-Hyslop, P.H., 2002. Gamma-secretase, Notch, Abeta and Alzheimer's disease: where do the presenilins fit in? Nat. Rev. 3, 281–290.

Tanzi, R.E., Bertram, L., 2005. Twenty years of the Alzheimer's disease amyloid hypothesis: a genetic perspective. Cell 120, 545–555.

Uemura, K., Lill, C.M., Li, X., Peters, J.A., Ivanov, A., Fan, Z., DeStrooper, B., Bacskai, B.J., Hyman, B.T., Berezovska, O., 2009. Allosteric modulation of PS1/gamma-secretase conformation correlates with amyloid beta(42/40) ratio. PLoS One 4, e7893.

Uemura, K., Farner, K.C., Hashimoto, T., Nasser-Ghodsi, N., Wolfe, M.S., Koo, E.H., Hyman, B.T., Berezovska, O., 2010. Substrate docking to gamma-secretase allows access of gamma-secretase modulators to an allosteric site. Nat. Commun. 1, 130.

Uemura, K., Farner, K.C., Nasser-Ghodsi, N., Jones, P., Berezovska, O., 2011. Reciprocal relationship between APP positioning relative to the membrane and PS1 conformation. Mol. Neurodegener. 6, 15.

Veeraraghavalu, K., Zhang, C., Miller, S., Hefendehl, J.K., Rajapaksha, T.W., Ulrich, J., Jucker, M., Holtzman, D.M., Tanzi, R.E., Vassar, R., et al., 2013. Comment on "ApoE-directed therapeutics rapidly clear beta-amyloid and reverse deficits in AD mouse models". Science (New York, NY) 340, 924-f.

Veeraraghavalu, K., Zhang, C., Zhang, X., Tanzi, R.E., Sisodia, S.S., 2014. Age-dependent, non-cell-autonomous deposition of amyloid from synthesis of beta-amyloid by cells other than excitatory neurons. J. Neurosci. 34, 3668–3673.

Wagner, S.L., Zhang, C., Cheng, S., Nguyen, P., Zhang, X., Rynearson, K.D., Wang, R., Li, Y., Sisodia, S.S., Mobley, W.C., et al., 2014. Soluble gamma-secretase modulators selectively inhibit the production of the 42-amino acid amyloid beta peptide variant and augment the production of multiple carboxy-truncated amyloid beta species. Biochemistry 53, 702–713.

Walsh, D.M., Klyubin, I., Fadeeva, J.V., Cullen, W.K., Anwyl, R., Wolfe, M.S., Rowan, M.J., Selkoe, D.J., 2002. Naturally secreted oligomers of amyloid beta protein potently inhibit hippocampal long-term potentiation in vivo. Nature 416, 535–539.

Wang, H., Sang, N., Zhang, C., Raghupathi, R., Tanzi, R.E., Saunders, A., 2015. Cathepsin L mediates the degradation of novel APP C-terminal fragments. Biochemistry 54, 2806–2816.

Ward, J., Wang, H., Saunders, A.J., Tanzi, R.E., Zhang, C., 2017. Mechanisms that synergistically regulate eta-secretase processing of APP and Aeta-alpha protein levels: relevance to pathogenesis and treatment of Alzheimer's disease. Discov. Med. 23, 121–128.

Welzel, A.T., Maggio, J.E., Shankar, G.M., Walker, D.E., Ostaszewski, B.L., Li, S., Klyubin, I., Rowan, M.J., Seubert, P., Walsh, D.M., et al., 2014. Secreted amyloid beta-proteins in a cell culture model include N-terminally extended peptides that impair synaptic plasticity. Biochemistry 53, 3908–3921.

Willem, M., Tahirovic, S., Busche, M.A., Ovsepian, S.V., Chafai, M., Kootar, S., Hornburg, D., Evans, L.D., Moore, S., Daria, A., et al., 2015. Eta-secretase processing of APP inhibits neuronal activity in the hippocampus. Nature 526, 443–447.

Zhang, C., 2012. Natural compounds that modulate BACE1-processing of amyloid-beta precursor protein in Alzheimer's disease. Discov. Med. 14, 189–197.

Zhang, C., 2017. Developing effective therapeutics for Alzheimer's disease—emerging mechanisms and actions in translational medicine. Discov. Med. 23, 105–111.

Zhang, C., Saunders, A.J., 2007. Therapeutic targeting of the alpha-secretase pathway to treat Alzheimer's disease. Discov. Med. 7, 113–117.

Zhang, C., Khandelwal, P.J., Chakraborty, R., Cuellar, T.L., Sarangi, S., Patel, S.A., Cosentino, C.P., O'Connor, M., Lee, J.C., Tanzi, R.E., et al., 2007. An AICD-based functional screen to identify APP metabolism regulators. Mol. Neurodegener. 2, 15.

Zhang, C., Browne, A., Child, D., Divito, J.R., Stevenson, J.A., Tanzi, R.E., 2010a. Loss of function of ATXN1 increases amyloid beta-protein levels by potentiating beta-secretase processing of beta-amyloid precursor protein. J. Biol. Chem. 285, 8515–8526.

Zhang, C., Browne, A., Child, D., Tanzi, R.E., 2010b. Curcumin decreases amyloid-beta peptide levels by attenuating the maturation of amyloid-beta precursor protein. J. Biol. Chem. 285, 28472–28480.

Zhang, C., Browne, A., Kim, D.Y., Tanzi, R.E., 2010c. Familial Alzheimer's disease mutations in presenilin 1 do not alter levels of the secreted amyloid-beta protein precursor generated by beta-secretase cleavage. Curr. Alzheimer Res. 7, 21–26.

Zoltowska, K.M., Maesako, M., Lushnikova, I., Takeda, S., Keller, L.J., Skibo, G., Hyman, B.T., Berezovska, O., 2017. Dynamic presenilin 1 and synaptotagmin 1 interaction modulates exocytosis and amyloid beta production. Mol. Neurodegener. 12, 15.